Available online at www.sciencedirect.com
SCIENCE DIRECT
ELSEVIER
Polymer 46 (2005) 5680–5688
polymer
www.elsevier.com/locate/polymer

Isothermal crystallization of isotactic polypropylene blended with low molecular weight atactic polypropylene. Part I. Thermal properties and morphology development

Jean-Hong Chen[a,*], Feng-Chou Tsai[a], Yu-Hsun Nien[a], Pei-Hung Yeh[b]

[a]*Department of Polymer Materials, Kun Shan University of Technology, Tainan 710, Taiwan, ROC*
[b]*Department of Industrial Engineering and Management, Diwan College of Management, Tainan 721, Taiwan, ROC*

Received 23 November 2004; received in revised form 10 March 2005; accepted 13 March 2005
Available online 8 June 2005

Abstract

The thermal properties and morphology development of isotactic polypropylene (iPP) homopolymer and blended with low molecules weigh atactic polypropylene (aPP) at different isothermal crystallization temperature were studied with differential scanning calorimeter and wide-angle X-ray scattering. The results of DSC show that aPP is local miscible with iPP in the amorphous region and presented a phase transition temperature at $T_c = 120$ °C. However, below this transition temperature, imperfect α-form crystal were obtained and leading to two endotherms. While, above this transition temperature, more perfect α- and γ-form crystals were formed which only a single endotherm was observed. In addition, the results of WAXD indicate that the contents of the γ-form of iPP remarkably depend both on the aPP content and isothermal crystallization temperature. Pure iPP crystallized was characterized by the appearance of α- and γ-forms coexisting. Moreover, the highest intensity of second peak, i.e. the (0 0 8) of γ-form coexisting with (0 4 0) of α-form, and crystallinity were obtained for blended with 20% of aPP, the γ-form content almost disappeared for iPP/aPP blended with 50% aPP content. Therefore, detailed analysis of the WAXD patterns indicates that at small amount aPP lead to increasing the crystallinity of iPP blend, at larger amount aPP, while decreases crystallinity of iPP blends with increasing aPP content. On the other hand, the normalized crystallinity of iPP molecules increases with increasing aPP content. These results describe that the diluent aPP molecular promotes growth rate of iPP because the diluent aPP molecular increases the mobility of iPP and reduces the entanglement between iPP molecules during crystallization.

Keywords: iPP/aPP blends; Morphology; Isothermal crystallization

1. Introduction

It is well known that isotactic polypropylene (iPP) exhibits several crystalline forms [1–15]. The α- or monoclinic-form is the most common and it occurs under conventional crystallization conditions [1]. The β- or hexagonal-form is substantially with a hexagonal lattice was recognized [2–5], and level of the β modification can be increased under specific conditions, such as temperature gradients, the presence of shearing forces, or occurs under β-nucleating agents are present [6–10]. The γ- or triclinic-form is least common, and is only observed in low molecular weight that have been promoted by hydrostatic pressures [4,11–15]. In all these structures of the conformation is identical and corresponds to the familiar threefold (3_1) helix, the various crystal morphologies being distinct through different stacking geometries of these helices. The thermal behaviors of iPP crystallized from the melt have been extensively studied. This is because the thermal behaviors are affected not only by molecular mass and molecular mass distribution, but also by different configuration and crystal morphologies, i.e. α-, β- and γ-crystal forms of iPP [16–26]. Interesting, a double endotherms occur at wide range temperatures, while only a single endotherm exists in the moderate crystallization temperature region. The origins for the double endotherms characteristics of iPP have been reported by Kawai [23]. They were indicated that it is a type of fractionation during

* Corresponding author. Tel.: +886 6 205 5138; fax: +886 6 205 0493.
E-mail address: kelvench@mail.ksut.edu.tw (J.-H. Chen).

0032-3861/$ - see front matter © 2005 Elsevier Ltd. All rights reserved.
doi:10.1016/j.polymer.2005.03.107

isothermal crystallization. Kim et al. [24] proposed the higher melting temperature due to a crystal fraction with molecular size higher than a critical value, while the lower melting temperature was generated when the molecular with high mobility crystallized on quenching after isothermal crystallization temperature. Hoffman et al. [25] attributed the double endotherms of iPP result from the lamellar thickening on annealing. On the other hand, Cox and Duswalt [26] concluded that the double endotherms at lower crystallization temperature originate from the transition of the metastable β-form into a stable α-form. While, Monasse and Haudin [27] observed that the double endotherms even for isothermal crystallized iPP showed only the α-form. Recently, Corradini et al. [28–30] concluded that the crystalline structure of the α-form may imply various degrees of disorder in the up and down positioning of the molecular, therefore, the double endotherms were the result of the ordered limiting structure, α_2, and a disordered limiting structure, α_1.

Polymer blends have received much attention for many decades because the morphology, crystallinity, microstructure, melting and crystallization behaviors of polymer blends are strongly dependence of the blend components [31–42]. Recently, the effect of aPP addition on the iPP has been investigated by Keith et al. [36,37]. They reported that with increasing aPP contain iPP/aPP blends, a more open spherulitic texture due to the incorporation of aPP diluent in the interfibrillar regions. Time resolved X-ray scattering techniques showed the relatively modest incorporation of aPP in the interlamellar regions depending on crystallization temperature and blend composition was reported by Wang et al. [33]. They indicated that the lamellar disorder and the size scale of lamellar were larger than the lamellar distance. The thermodynamic miscibility of iPP and aPP has also received attention [38–40]. The aPP component is reported to be miscible with iPP in the molten state from the evaluation of an equation of state theory using low molecular weight aPP [39]. However, aPP has also been reported to be immiscible with iPP in the solid state, as observed by transmission electron microscopy (TEM) when the aPP sample has a high M_w and a narrow molecular weight distribution [40]. Thus, a fundamental understanding of the miscibility of the components is in one phase or in multiple phases with specific interaction with each other in the amorphous region of blends. Therefore, the morphology of polymer blends is even more complicated since the liquid–solid demixing and liquid–liquid phase separation of the components in blends during crystallization.

In this study, we attempt to correlate the crystallization and melting behaviors of isotactic polypropylene blended with low molecular mass but similar molecular mass distribution of atactic polypropylene. The crystallization and melting behaviors of iPP and blends have been investigated by DSC and WAXS. The dependence of thermal properties and crystallized morphology of iPP blends on the both aPP content and isothermal crystallization temperature will be discussed.

2. Experimental

2.1. Materials

The isotactic polypropylene (Aldrich 42785-3) with a weight-average molecular weight of $M_w = 5.8 \times 10^5$ g mol^{-1} and atactic polypropylene (Aldrich 42818-3) with $M_w = 1.96 \times 10^4$ g mol^{-1}, respectively, were supplied by Aldrich Chemical Co. Ltd, used in this work was a laboratory grade samples. Melt-blended specimens of these homopolymers with various compositions were prepared by a twinscrew apparatus (MP2015 APV Chemical Machinery Co. Ltd, USA) at 210 °C. The mixing ratios of iPP/aPP (wt/wt): 100/0, 90/10, 80/20, 70/30, 50/50 and 30/70 were prepared and defined as iPP-100, iPP-90, iPP-80, iPP-70, iPP-50, and iPP-30. The composition and the properties of blends that have been used in this study are compiled in Table 1.

2.2. Preparation of compression-molded samples

The compression-molded films was prepared by melt-pressing of different iPP/aPP blends for a molding of $120 \times 120 \times 1$ mm^3, placed between a pair of steel platens, at temperature was 210 °C and 10 min holding time, the iPP/aPP blended film was taken out and immediately submerged in a temperature controlled compression molding machine at T_c,the temperatures of 5 °C intervals starting from 90 to 130 °C, under a pressure of 50 kg cm^{-2}, where it was still between the two steel platens holding 120 min. This treatment assumes that previous thermal and mechanical histories were essentially erased and provides a controlled condition for the film.

2.3. Thermal behavior of iPP/aPP blended samples

All the iPP/aPP blended samples in Table 1 were measured the crystallization and melting behaviors with a differential scanning calorimeter (PYRIS Diamond DSC with an intra-cooler for lowermost temperature about −65 °C). Sample weight about 5 mg was cut from the blended specimen and put into sample pan and then melted in the furnace in a nitrogen atmosphere at 210 °C for 10 min, followed by cooling at a rate of 10 °C min^{-1} and the crystallization thermogram was measured. The temperature of peak and area of the exothermic curve were taken as the crystallization temperature, T_c, and the latent heat of crystallization, ΔH_c, respectively. As soon as the temperature reached −50 °C, it was reheated again at a rate of 10 °C min^{-1} and the melting thermogram was measured. The glass transition temperature, T_g, and temperature of peak and area of the endothermic curve were taken as the melting temperature, T_m, and the heat of fusion, ΔH_f, respectively. These measurement results are shown in Table 1.

Table 1
Molecular characteristic of the PP samples

Sample	Type	Isotacticity	M_w	M_w/M_n	T_m (°C)	T_g (°C)
IPP	Isotactic	95.3[a]	580,000	3.5	163.2[b]	−10.1[c]
APP	Atactic	–	19,600	3.5	–	−14.6[c]

[a] From ^{13}C NMR (mm%).
[b] From melting endotherm of DSC trace.
[c] From DSC trace.

2.4. Thermal behavior of isothermal crystallized iPP/aPP blended samples

About 5 mg iPP blended samples after isothermal crystallization were heating at a rate of 10 °C min^{-1} in the furnace in a nitrogen atmosphere and the melting thermogram was also measured.

2.5. Wide-angle X-ray diffraction

Wide-angle X-ray diffraction (WAXD) intensity curves of iPP blends were measured with a graphite-monochromatized Cu K_α radiation generated at 40 kV and 180 mA in a Rigaku D/max diffractometer. WAXD intensities were recorded from $2\theta = 5$–$35°$ with a continuous scanning speed of $2\theta = 1° \text{ min}^{-1}$ with data collection at each 0.05° of 2θ was performed.

3. Results and discussion

3.1. Thermal behavior of iPP/aPP blended samples

The crystallization and melting behaviors of iPP homopolymer and iPP blended with low molecular weight aPP were investigated by DSC is shown in Figs. 1 and 2. The crystallization and remelting curves of iPP/aPP blends were melted at 210 °C for 10 min, followed by cooling at a rate of 10 °C min^{-1} to −50 °C, when the temperature reached −50 °C, it was remelting again at a rate of 10 °C min^{-1}. These thermograms are characterized by both a single peak at crystallization and remelting traces. The single melting endothermic and crystallization exothermic characteristics may be due to presence of a α-form crystal of iPP in iPP blends. The melting temperature, T_m, heat fusion of melting, ΔH_f, crystallization temperature, T_c, and latent heat of crystallization, ΔH_c, respectively, of iPP blends all decrease evidently with increasing aPP content (shown in Table 2). Recently, the phase morphology of iPP/LLDPE polymer blended has been performed by Li et al. [42–44]. They reported that decreases the crystallization rate of iPP/LLDPE blended might be due to two reasons. The first is that iPP in PE can be viewed as iPP in solution, and the iPP nucleation is reduced [43,44]. The second is that the viscous LLDPE slows the diffusion of iPP chains during crystallization [44]. This results of Figs. 1 and 2 indicate that the crystallization ability and crystal morphology of iPP is strong function of aPP content because the nucleation and growth rates of crystallization behavior for iPP is be interrupted with aPP molecules. The thermal properties and morphology of iPP strongly depend on the miscibility

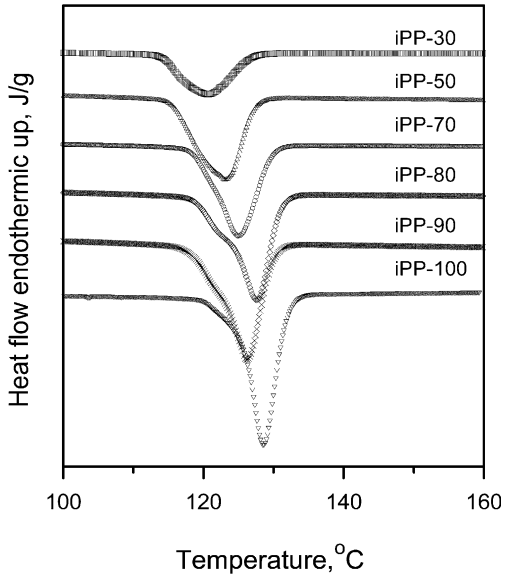

Fig. 1. Influence of aPP contents on the crystallization exotherm of iPP blends after molten.

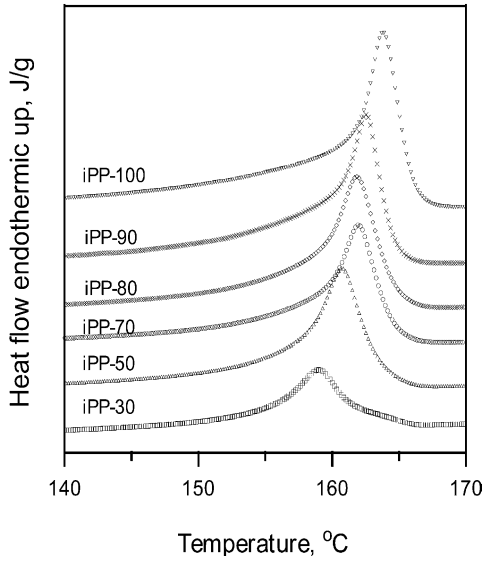

Fig. 2. Influence of aPP contents on the melting endotherms of iPP blends after crystallization.

Table 2
Thermal properties of the iPP/aPP blend samples

Materials	T_g (°C)	T_c (°C)	ΔH_c (J/g)	T_m(°C)	ΔH_f (J/g)
iPP-100	−10.1	129.0	83.7	163.2	85.1
iPP-90	−10.1	126.1	78.8	162.5	78.9
iPP-80	−10.3	127.6	72.6	161.5	74.0
iPP-70	−10.6	125.1	61.7	160.6	63.1
iPP-50	−10.4	123.1	62.7	158.7	64.6
iPP-30	−11.1	120.6	33.4	156.9	36.0
iPP-0	−14.6	–	–	–	–

between the iPP and aPP in the blend. Thus, a fundamental understanding of the miscibility of the components is in one phase for the amorphous region of blends. Therefore, the miscibility between the iPP and aPP molecules in the amorphous region of iPP blended will be discussed below. Recently, the thermal behavior of sPP mixture with aPP using DSC and WAXD has reported by Phillips and Jones [41]. They indicated that the addition of aPP leads to a suppression of crystallization temperature, and promotion endotherm II on heating. Both behaviors suggested a degree of 'local' mixing of diluent within the morphology. Fig. 3 shows the glass transition temperature, T_g, of iPP blends as a function of aPP content at heating rate of 10 °C min^{-1}. However, a general feature of these curves are appeared of a single transition or one phase behavior in iPP blends and decrease slightly with increasing aPP content (as shown in Table 2) [39]. Therefore, the result indicates that the aPP molecular is miscible with iPP molecular in the amorphous region, this may be implying the configuration of uncrystallize sequence of iPP is same as of sequence of aPP in the amorphous region.

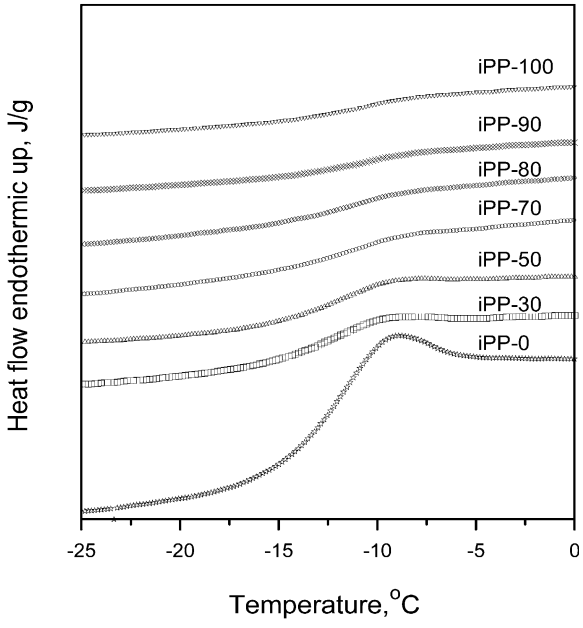

Fig. 3. Influence of aPP contents on the T_g of iPP blends after crystallization.

3.2. Thermal behavior of isothermal crystallized of iPP/aPP blended samples

Fig. 4(a)–(f) shows the DSC melting scans at a heat rate of 10 °C min^{-1} for isothermal crystallized iPP blends at different isothermal crystallization temperature. However, a general feature of these curves is the appearance of two melting endotherms at temperature below 120 °C, while shows a single melting endotherm at temperature above 120 °C [23,24]. It is observed that by increasing the aPP content, the heat fusion of the lower-temperature endotherm, ΔH_f^L, decreased, while the heat fusion of the higher-temperature endotherm, ΔH_f^H, increased. The heat fusion and morphology of the two endotherms were found to be dependent on the aPP content and isothermal temperature, so the crystallinity and morphology of iPP blends after isothermal crystallization is also affected by the aPP content and by the isothermal crystallization temperature. Wang et al. concluded that the predominantly interfibrillar incorporation of the aPP diluent within the microstructure with only dependent on the crystallization temperature [33]. The decrease in ΔH_f^L with increasing aPP content is indicative of reducing recrystallization or reorganization of the crystals originally formed during crystallization. Therefore, the ΔH_f^L usually represents the melting of the crystals formed during crystallization, while the ΔH_f^H is probably due to the melting of crystals of higher stability formed by the recrystallization of crystals initially obtained. Moreover, the area of the ΔH_f^L increases with increasing isothermal temperature, because a higher degree of perfection was achieved in the crystals initially obtained. While the area of the ΔH_f^H decreases with increasing isothermal temperature. This is due to the melting of crystals formed during recrystallization, and the results obtained can be assumed because the same degree of perfection is achieved in recrystallized crystals. This result as discussed by Corradini et al., however, the double endotherms may be attributed to the recrystallization of less ordered, α_1, form with a random distribution of up and down chain packing with methyl groups to a more ordered, α_2, form with a well-defined deposition of up and down helices in the unit cell [28–30]. The ΔH_f^L and melting temperature of lower-endothermic, T_m^L, remains almost constant at temperature below 105 °C, and then increase ΔH_f^L and T_m^L at higher isothermal temperature. By increasing the isothermal temperature or

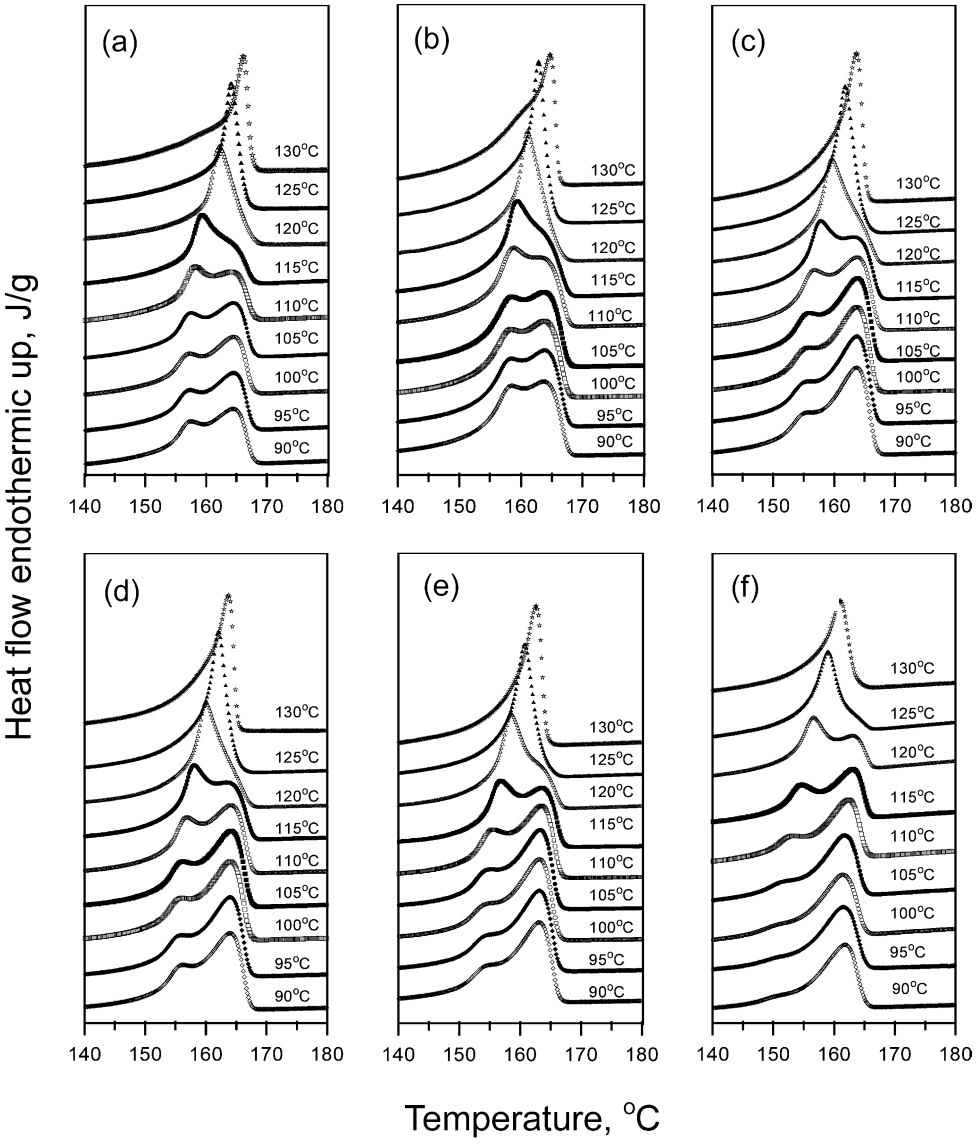

Fig. 4. Melting endotherms of iPP blends after isothermal crystallization for 120 min at different isothermal temperatures: (a) iPP-100, (b) iPP-90, (c) iPP-80, (d) iPP-70, (e) iPP-50, and (f) iPP-30.

decreasing the supercooling temperature, higher T_m^L was observed. This is indicating that a higher degree of perfection is achieved in the crystals due to the higher thermodynamic mobility of iPP molecular for the recrystallization to take place. The ΔH_f^L and T_m^L do not change at temperature below 105 °C implying the previous thermal history or degree of perfection achieved may be the same. The melting temperature of higher-endothermic, T_m^H, remains unchanged while the ΔH_f^H decreases with increasing isothermal crystallization temperature. Increasing the crystallization temperature led to promotion a higher degree of perfection of crystals and less of iPP chain for the recrystallization to take place at higher temperatures, so the obtained crystals are more perfect than those formed at lower isothermal temperature. Isothermal temperature causes the distributions of two melting endotherms of iPP have been previously reported [18,24–29].

For all isothermal crystallization temperatures investigated, the iPP blends showed two melting endothermic are observed at isothermal crystallization temperature below 120 °C, while a single endothermic peak is observed at isothermal crystallization temperature above 120 °C. This result could be attributed to two different iPP crystal-forms as discussed below. In fact, the iPP crystallizes at different isothermal crystallization temperatures from molten suggested that simultaneously crystallizes in both the α- and the γ-form of iPP. The observed melting temperature of the lower-endothermic, T_m^L, linearly increases with the crystallization temperature for iPP blended. To determine the equilibrium melting temperature, T_m°, recorded using the

Hoffmann–Weeks equation [45], a plot of T_c versus T_m with a line is drawn, where $T_c = T_m$. The experimental data can be extrapolated to the intersection with the line, the intersection is the T_m^0 as following relation:

$$T_m^0 - T_m = \phi'(T_m^0 - T_c) \quad (1)$$

where ϕ' represents a stability parameter that depends on crystal size and perfection, T_m^0 is the equilibrium melting temperature. Fig. 5 shows the melting temperatures registered at the maximum of the peak relative to the T_m^L for the isothermally crystallized iPP blends. A straight line was extrapolated from the experimental T_m^L values of iPP blends, and the calculated equilibrium melting temperature, T_m^0, for all iPP blends was observed. Fig. 6 shows the effect aPP content on the T_m^0 of iPP blends. The result illustrates that the T_m^0 decrease slightly at aPP content below 30% (iPP-70), while decrease remarkably at aPP content above 50% (iPP-50). The T_m^0 of pure iPP (iPP-100) and iPP-30 blend is equal to 187.2 and 181.6 °C, respectively, is observed. These values are agree with the thermal properties of iPP is strongly function of aPP content as discussed above.

3.3. Morphology development of isothermal crystallized of iPP/aPP blended samples

WAXD intensity curves of iPP blends after isothermal crystallization at temperature is 110 and 130 °C, respectively, as shown in Figs. 7 and 8. The X-ray diffractograms of samples of iPP blends show nearly the α-form diffractograms after isothermally crystallized at 110 °C. For iPP isothermally crystallized at 110 °C, the characteristic peaks of the α-form can be found at 2θ angles of 14.08° (1 1 0), 16.95° (0 4 0), 18.5° (1 3 0), 21.2° (1 1 1), and 21.85° (−1 3 1 and 0 4 1) as diffraction are marked of iPP-30 in Figs. 7 and 8

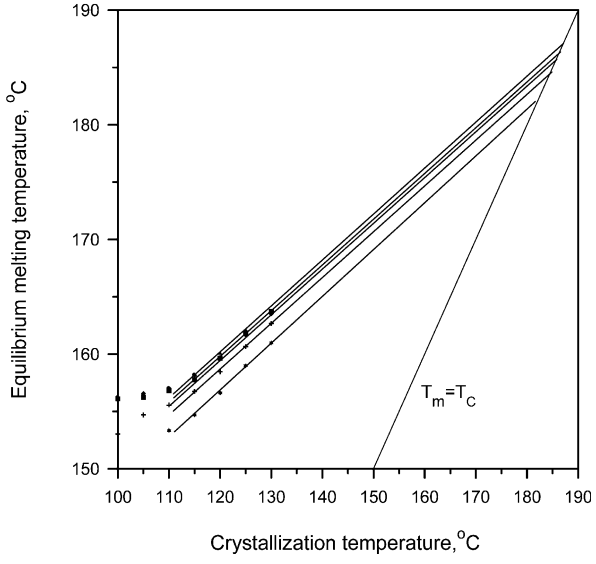

Fig. 5. A plot of the observed melting temperature of the lower endothermic versus the crystallization temperature recorded using the linear Hoffman–Weeks extrapolation.

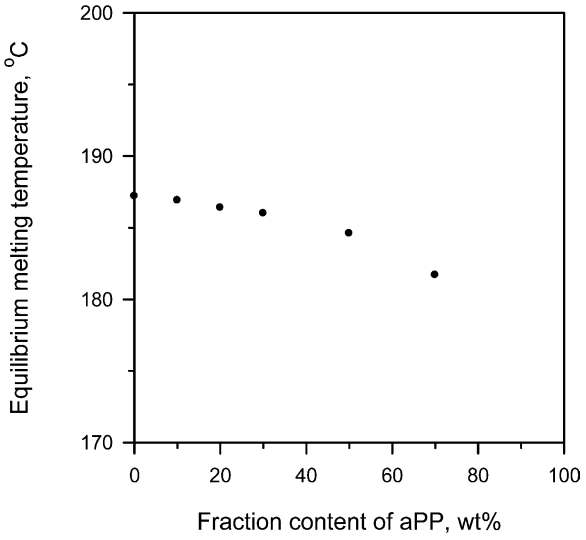

Fig. 6. The equilibrium melting temperature (T_m^0) as a function of the aPP content.

[46]. However, the typical WAXD intensity pattern of the α-form, the intensity of second peak (0 4 0) must be smaller than the first one peak (1 1 0). The WAXD intensity curves show an unusually pattern, i.e. the intensity of second peak is stronger than the first one peak. Although, this effect aPP content on iPP blends at 110 °C is not observed in samples containing the γ-form of identification peak at $2\theta = 20.07°$. The characteristic peaks of the presence of γ-form of iPP usually can be found at 2θ angles of 13.84° (1 1 1), 15.05° (1 1 3), 16.72° (0 0 8), 20.07° (1 1 7), 21.2° (2 0 2), and 21.88° (0 2 6) [47]. On the other hand, the γ-form of iPP observed evidently in the iPP-100 sample at isothermal crystallization temperature above 120 °C as shown in Figs. 8 and 11. These

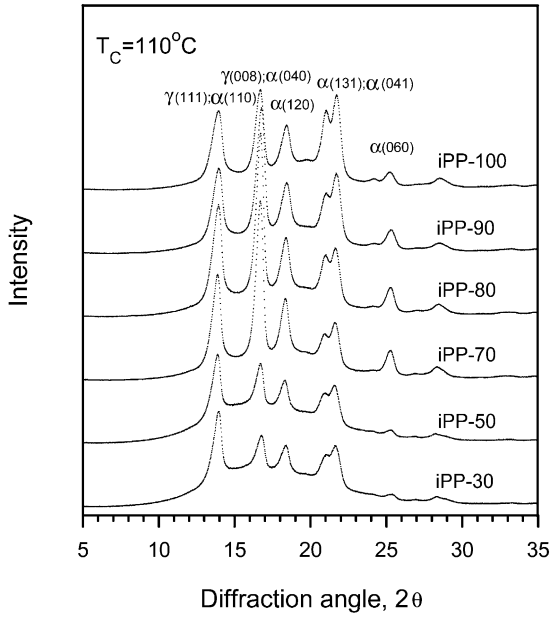

Fig. 7. WAXD intensity patterns of iPP blends after isothermal crystallization for 120 min at 110 °C.

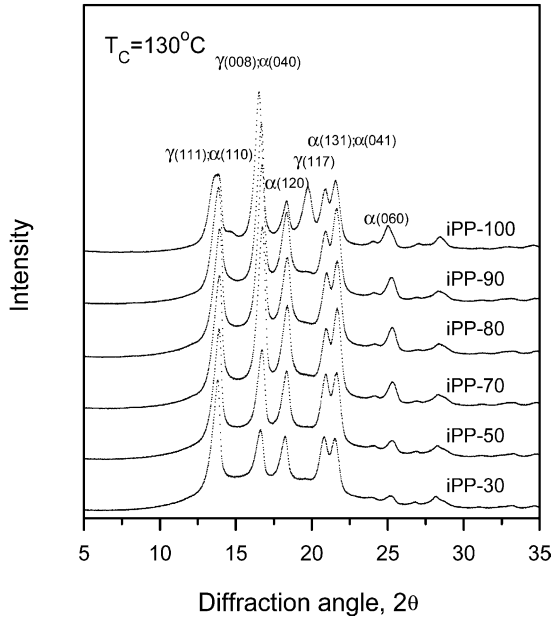

Fig. 8. WAXD intensity patterns of iPP blends after isothermal crystallization for 120 min at 130 °C.

patterns are characterized by the second peak is larger than the first one and show a peak of γ-form (1 1 7) at $2\theta = 20.07°$. This result indicates that the location of the strong second peak then the first one may be due to the (0 0 8) of γ-form coexisting with (0 4 0) of α-form, implying a lower degree of perfection of γ-form crystals coexisting with the α-form of iPP during crystallization. This is interesting that aPP content even in small amounts, lead to reducing the γ-form crystallization; that is disappear the (1 1 7) peak at $2\theta = 20.07°$. While, increasing the α- to γ-form crystal transition of iPP, i.e. at small amounts of aPP, the second peak is higher than the first one, and overall crystallinity higher than the iPP homopolymer. The developing intensity of second peak explain that the aPP molecular arises a diluent affection on the growth rate of γ-form crystallize because the diluent aPP molecular promotion the mobility of iPP and suppression the entanglement between iPP molecules. On the other hand, when aPP content is above 50 wt%, the diffraction pattern shows only the α-form diffractogram.

WADX can be used to measure the crystallinity, X_c, from the ratio of the areas under the crystalline and amorphous diffractions, A_{cr} and A_{am} as shown in Fig. 9

$$X_c = \frac{K_{cr}A_{cr}}{K_{cr}A_{cr} + K_{am}A_{am}} \quad (2)$$

where K_{cr} and K_{am} are constants normally assumed to be equal. X_c was calculated in each case with above equation and assuming $K_{cr} = K_{am}$. The accuracy of these results is limited by difficulties in estimating the contribution of the amorphous background [50]. Fig. 10(a) and (b) show the effect of aPP content on the crystallinity of iPP blended and the normalized crystallinity of iPP within iPP blends, respectively. With increasing aPP content, the crystallinity

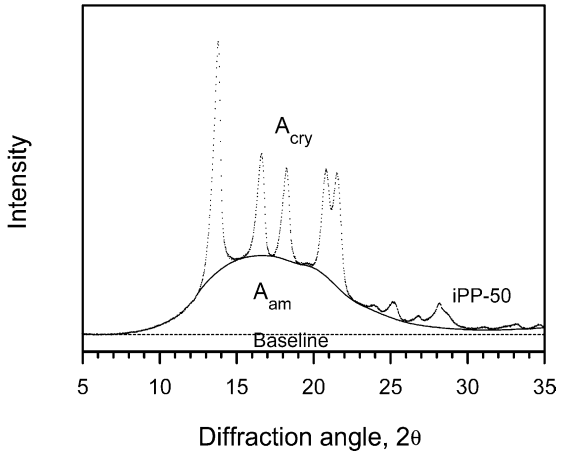

Fig. 9. Calculation methods for crystallinity of iPP blended by WAXD diffractograms.

of iPP blended increased and then decreasing. This result, as expected above, indicates that the crystallization ability of iPP is strong function of aPP content. At small amounts of aPP, the crystallinity of iPP blends higher then that of pure iPP. The developing the crystallinity of iPP blend explain that the diluent aPP molecular suppression the entanglement between iPP molecules and promotion the mobility of iPP molecular during crystallization. While, at larger amounts of aPP, decreasing the crystallinity of iPP blends may be due to the larger amount diluent aPP action more suppress the concentration of nucleus and inhibits the iPP molecular diffusing to a surface of nucleus during crystallization. On the other hand, aPP is a non-crystalline polymer, which blended with iPP homopolymer can acting as a diluent or plasticizer. Therefore, Fig. 10(b) shows the normalized crystallinity or crystallizability of iPP chain within iPP blended. The normalized crystallinity was calculated with

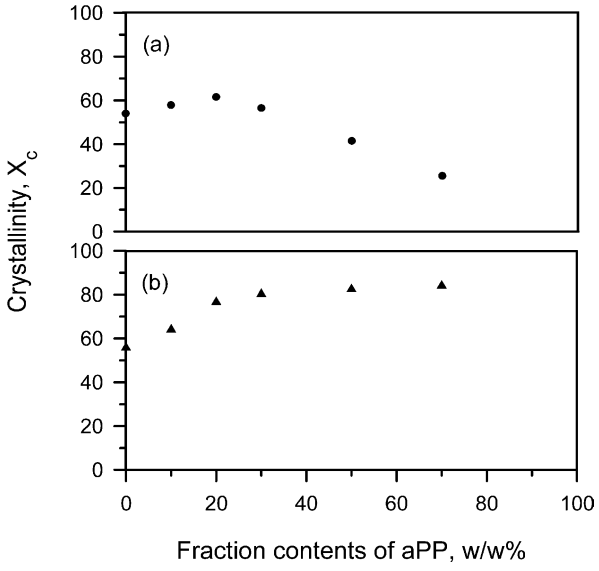

Fig. 10. Effect of aPP contents on (a) the crystallinity of iPP blends, (b) the normalized crystallinity of iPP within iPP blends.

the result of crystallinity of iPP blends divided by iPP content within iPP blended. This result shows that the normalized crystallinity of iPP molecules within iPP blend increases with increasing aPP content. This result describes that the aPP molecular promotes the growth rate of iPP because the diluent aPP molecular increasing the mobility of iPP and reducing the entanglement between iPP molecules lead to increasing the normalized crystallinity of iPP during crystallization.

The dependent the morphology development of iPP-100 on the different isothermal temperature will discuss on Fig. 11. Fig. 11 shows the WAXD intensity curves of iPP-100 at various isothermal crystallization temperatures for 120 min. As the isothermal crystallization temperature increases the γ-form crystals increased [14]. The results of WAXD intensity curves indicate that at higher isothermal temperature, i.e. lower supercooling, were shown to be more favorable for γ-form growth of iPP. Recently, the ratio of γ-form was calculated simply from the relative intensities of the unique γ- and α-form peaks at $2\theta = 20.07$ and 18.58°, respectively [48,49]. Therefore, in this study the overall intensities in the 2θ ranges between 17.5 and 20.2 of WAXD intensity curves are determined. After subtraction of background scattering, the intensity of the γ-form is obtained directly from WAXD intensity curves. The fraction contents of all other peaks are then calculated on the basis of the relative area of peak as below equation:

$$F_{\gamma-\text{form}} = \frac{A_{20.07}}{A_{20.07} + A_{18.58} + A_{\text{am}}} \quad (3)$$

$$F_{\alpha-\text{form}} = \frac{A_{18.58}}{A_{20.07} + A_{18.58} + A_{\text{am}}} \quad (4)$$

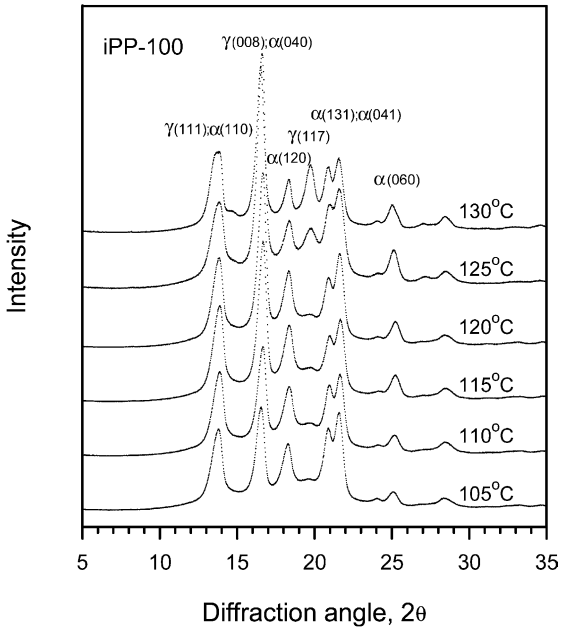

Fig. 11. WAXD intensity patterns of iPP-100 at various isothermal crystallization temperatures for 120 min.

where $A_{20.07}$, $A_{18.58}$, and A_{am} are area of peaks located at 20.07 and 18.58°, respectively, and area of amorphous. The $F_{\gamma\text{-form}}$ is area of the peak of γ-form for (1 1 7) plane at 20.07° is divided by the sum of the areas of all peaks of 18.58, 20.07 and area of amorphous as Eq. (3). The F_{am} is unity minus phase functions of $F_{\gamma\text{-form}}$ and $F_{\alpha\text{-form}}$. These rationales are adopted throughout this work to evaluate quantitatively the amount of α- and γ-form relationship with isothermal temperature. The above method fails for some amounts of γ-form when the crystal peaks were not distinguished accurately from the amorphous background. Fig. 12 shows the dependence of phase fraction of various crystals on the isothermal crystallization temperature. As isothermal crystallization temperature increased, the fraction content of γ-form increasing remarkably from about 2 to 34.2%, while fraction content of α-form and amorphous decreasing from 33.1 to 21.3% and 65.2 to 44.1%, respectively. The α-form decreases explicitly at temperature above 120 °C. Contrary, the γ-form increases remarkably at temperature above 120 °C. This result indicates that at higher isothermal temperature, i.e. lower supercooling, shows to be more favorable for γ-form growth in iPP-100. Increasing the crystallization temperature was promoted a α- to γ-form transition and inducing a higher degree of perfection of γ-form crystals are observed. The γ-form crystals for (1 1 7) are more perfect than those formed at lower isothermal temperature, i.e. the stronger intensity of second peak (0 0 8) as discussed above.

4. Conclusions

The thermal properties and morphology development of isotactic polypropylene homopolymer and blended with low molecular weight atactic polypropylene at different isothermal crystallization temperature were observed. The results can be summarized as follows: (a) the aPP is miscible with iPP in the amorphous region, (b) aPP amounts lead to

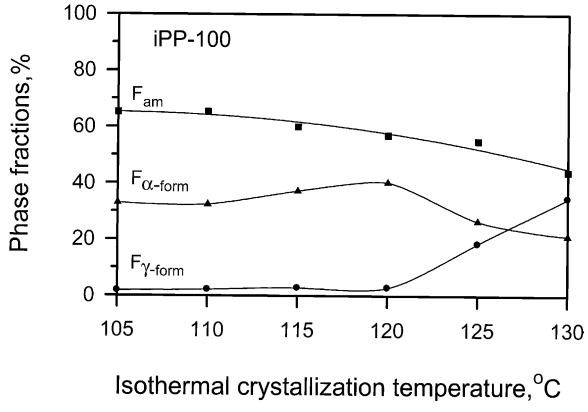

Fig. 12. Amount of the (●) $F_{\alpha\text{-form}}$, (▲) $F_{\gamma\text{-form}}$, and (■) F_{am} phase fractions determined by analysis of the areas of peaks at 18.58, 20.07 and amorphous of iPP-100 at various isothermal crystallization temperatures for WAXD diffractograms.

the formation of α-form of iPP in iPP and blends, (c) increases the crystallinity of iPP blend at small amount aPP, while decreases crystallinity with increasing larger amount aPP, (d) increasing the normalized crystallinity of iPP molecular within blend as aPP content increased, (e) isothermal crystallization temperature lead to enhance the amount of γ-form formed in pure iPP and iPP blends. The contents of the γ-form of iPP remarkably depend both on the aPP content and isothermal crystallization temperature. Pure iPP crystallized was characterized by the appearance of α- and γ-forms coexisting. The higher intensity of second peak and crystallinity were obtained for blended with 20% of aPP, the γ-form content decreased and almost disappeared for iPP/aPP blends with 50% aPP content. This behavior suggested that the lower γ-nucleation rate and higher density of α-nuclei occurs at the early stage of crystallization for iPP blends. In iPP blends, both α- and γ-forms obtained after isothermal crystallization showed a strong tendency to recrystallization or reorganization, and double melting endotherms were observed during the heating process. This trend is due to the imperfect crystal formed during the crystallization.

The α- and γ-forms obtained after isothermal crystallization at different temperatures exhibited single or double melting endotherms in the subsequent heating process, depending on the crystallization temperature. The presented a α- to γ-forms transition temperature at $T_c = 120$ °C. At crystallization temperatures lower than this transition temperature, imperfect α- and γ-form crystals were obtained and recrystallization or reorganization took place, leading to two endotherms. Above this transition temperature, more perfect α- and γ-form crystals were formed which were not susceptible to recrystallization or reorganization, and only a single endotherm was observed. Samples containing only the α-form heated after isothermal crystallization temperature showed two lower melting endotherms due to α-form recrystallization was smaller because of the occurrence of certain α-form recrystallization.

Acknowledgements

The authors gratefully acknowledges the financial support of National Science Council of the Republic of Chain through project NSC 91-2216-E168-002 and gratefully the research facility of WAXD provide by the Nanotechnology R&D Center of Kun Shan University of Technology.

References

[1] Natta G, Corradini P. Nuovo Cimento Suppl 1960;15:40.
[2] Padden FJ, Keith HD. J Appl Phys 1959;30:1479.
[3] Keith HD, Padden FJ, Walter NM, Wycoff MW. J Appl Phys 1959;30:1479.
[4] Turner-Jones A, Aizlewood JM, Beckett DR. Makromol Chem 1964;75:134.
[5] Turner-Jones A, Cobbold AJ. J Polym Sci 1968;6:539.
[6] Stocker W, Schumacher M, Graff S, Thierry A, Wittmann JC, Lotz B. Macromolecules 1998;31:807.
[7] Norton DR, Keller A. Polymer 1985;26:704.
[8] Jacoby P, Bersted BH, Kissel WJ, Smith CE. J Polym Sci, Part B: Polym Phys Ed 1986;24:461.
[9] Varga J, Karger-Kocsis J. J Polym Sci, Polym Phys Ed 1996;34:657.
[10] Samuels RJ, Yee RY. J Polym Sci, A-2 1972;10:385.
[11] Morrow DR, Newman BA. J Appl Phys 1968;39:4944.
[12] Kardos JL, Christiansen AW, Bear E. J Polym Sci, A-2 1966;4:777.
[13] Campbell RA, Phillips PJ, Lin JS. Polymer 1993;34:4809.
[14] Mezghani K, Phillips PJ. Polymer 1997;38:5725.
[15] Mezghani K, Phillips PJ. Polymer 1998;39:3735.
[16] Zhu XY, Yan DY, Tan SS, Wang T, Yan DH, Zhou EL. J Appl Polym Sci 2000;77:163.
[17] Paukkeri R, Lehtinen A. Polymer 1993;34:4083.
[18] Caldas V, Brown GR, Nohr RS, Macdonald JG. J Polym Sci, Polym Phys Ed 1996;34:2085.
[19] Yoshida H. Thermochim Acta 1995;267:239.
[20] Fillon B, Thierry A, Wittmaan JC, Lotz B. J Polym Sci, Polym Phys Ed 1993;31:1407.
[21] Fillon B, Wittmaan JC, Lotz B, Thierry A. J Polym Sci, Polym Phys Ed 1993;31:1383.
[22] Marco C, Gómez MA, Ellis G, Arribas JM. J Appl Polym Sci 2002;84:1669.
[23] Kawai T. Makromol Chem 1965;84:290.
[24] Kim YC, Ahn W, Kim CY. Polym Eng Sci 1997;7:309.
[25] Hoffman JD, Weeks JJ. J Chem Phys 1965;42:4301.
[26] Cox WW, Duswalt AA. Polym Eng Sci 1967;7:309.
[27] Monasse B, Haudin JM. Colloid Polym Sci 1985;263:822.
[28] Corradini P, Napolitano R, Oliva L, Petraccone V, Pirozzi B. Makromol Chem Rapid Commun 1982;3:753.
[29] Rosa CD, Guerra G, Napolitano R, Petraccone V, Pirozzi B. Eur Polym J 1984;20:937.
[30] Guerra G, Petraccone V, Corradini P, Rosa CD, Napolitano R, Pirozzi B, et al. J Polym Sci, Polym Phys Ed 1984;22:1029.
[31] Wang ZG, Phillips RA, Hsiao BS. J Polym Sci, Polym Phys Ed 2000;38:2580.
[32] Phillips RA. J Polym Sci, Polym Phys Ed 2000;38:1947.
[33] Wang ZG, Phillips RA, Hsiao BS. J Polym Sci, Polym Phys Ed 2001;39:1876.
[34] Foresta T, Piccarolo S, Goldbeck-Wood G. Polymer 2001;42:1167.
[35] Torre J, Cortázar M, Gómez M, Ellis G, Marco C. J Polym Sci, Polym Phys Ed 2004;42:1949.
[36] Keith HD, Padden FJ. J Appl Phys 1964;35:1270.
[37] Keith HD, Padden FJ. J Appl Phys 1964;35:1286.
[38] Lohse D. Polym Eng Sci 1986;26:1500.
[39] Maier RD, Thomann R, Kressler J, Mulhaupt R, Rudolf B. J Polym Sci, Polym Phys Ed 1997;35:1135.
[40] Silvestri R, Sgarzi P. Polymer 1998;39:5871.
[41] Phillips RA, Jones RL. Macromol Chem Phys 1999;200:1912.
[42] Li J, Shanks RA, Long Y. J Appl Polym Sci 2001;82:628.
[43] Li J, Shanks RA, Olley RH, Greenway GR. Polymer 2001;42:7685.
[44] Li J, Shanks RA, Long Y. Polymer 2001;42:1941.
[45] Hoffman JD, Weeks JJ. J Res Natl Bur Stand 1962;66A:13.
[46] Phillips RA, Wolkowicz MD. In: Moore EP, editor. Polypropylene handbook. Hanser: Munich, 1996. p. 113 [Munich].
[47] Varga J. J Mater Sci 1992;27:2557.
[48] Mezghani K, Phillips PJ. Polymer 1995;36:2407.
[49] Zimmermann HJ. J Macromol Sci, Phys B 1993;32(2):141.
[50] Feng J, Jin X, Hay JN. J Appl Polym Sci 1998;68:381.